Agricultural Water Management 275 (2023) 107994

Contents lists available at ScienceDirect

Agricultural Water Management

journal homepage: www.elsevier.com/locate/agwat

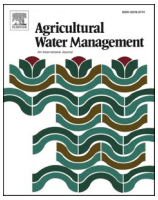

Optimizing fertigation schemes based on root distribution

Wenjie Meng [a], Jinliang Xing [a], Mu Niu [a], Qiang Zuo [a], Xun Wu [a], Jianchu Shi [a,b,*], Jiandong Sheng [b], Pingan Jiang [b], Quanjia Chen [c], Alon Ben-Gal [d]

[a] College of Land Science and Technology, China Agricultural University; Key Laboratory of Plant-Soil Interactions, Ministry of Education; and Key Laboratory of Arable Land Conservation in North China, Ministry of Agriculture and Rural Affairs, Beijing 100193, China
[b] College of Resources and Environment, Xinjiang Agricultural University, Urumqi 830052, China
[c] College of Agricultural Science, Xinjiang Agricultural University, Urumqi 830052, China
[d] Soil, Water and Environmental Sciences, Agricultural Research Organization-Volcani Institute, Gilat Research Center, Mobile post Negev, 85280, Israel

ARTICLE INFO

Handling Editor - Xiying Zhang

Keywords:
Fertigation scheduling
Normalized root length density
Nutrient transport
Root nutrient uptake
Drip-irrigated cotton under film mulch

ABSTRACT

When fertigation is applied, fertilizer is often injected into drip irrigation systems according to a single-pulse application method (SPAM) where a single dose is given either in the early, middle, or late stage of an irrigation event. To improve the consistency of distributions between nutrients and roots and thus promote root nutrient uptake, a root distribution-based multistage application method (RMAM) was proposed, where fertilizer was injected in stages during each irrigation event and proportionally according to the distribution of normalized root length density. A case study to verify the potential of RMAM and to test it against other fertigation scheduling strategies was conducted in a two-year field experiment with drip-irrigated cotton under film mulch in Xinjiang, China. Results indicated fertilizer application strategies significantly impacted soil nutrient dynamics. Generally, SPAM caused nutrient accumulation in certain soil layers, while uniform multistage application method (UMAM) resulted in a more even nutrient profile. Optimal nutrient profile for root uptake was obtained by RMAM, where more nutrients were located in the upper soil layers containing more roots. Compared to late-stage SPAM, the best among all the schemes of UMAM and SPAM, RMAM did not influence deep leaching of mineral N and available P, but did reduce leachate of available K by an average of 3.5% during the fertigation periods over the two seasons. Furthermore, at the late boll-opening stage, due to 25.8%, 35.7% and 35.3% increases of average aboveground accumulation (representing root nutrient uptake) for N, P and K, average soil residual respectively decreased 23.8%, 6.2% and 3.1%, and average cotton yield enhanced 5.5%. Besides root length density, crop nutrient uptake is also affected by many other complicated factors such as soil water/nutrient dynamics and root uptake activity, and thus RMAM should be further investigated to consider these factors comprehensively.

1. Introduction

In arid and semi-arid regions with unavoidable water and salinity stresses, crops are often subject to limited soil nutrient availability (Chen et al., 2010; Wang et al., 2018). Sustainable agricultural production in these areas therefore pursues how to improve root zone soil environmental conditions and thus to increase water and fertilizer use efficiencies. In the last decades, water-saving irrigation, especially drip irrigation, has been developed worldwide with a rapidly increasing application area. Due to its contribution to saving water and fertilizer, mitigating salinization impact, and enhancing crop yield, film-mulched drip irrigation has gained popularity. Furthermore, when it is utilized for nutrient management (fertigation), its contribution to sustainable agricultural development accentuated (Ning et al., 2021; Zong et al., 2021).

Nutrient distribution and root uptake are expected to be functions of the interaction between soil water flow and solute transport in a system, in which nutrients are injected into irrigation pipe network and

* Corresponding author at: College of Land Science and Technology, China Agricultural University; Key Laboratory of Plant-Soil Interactions, Ministry of Education; and Key Laboratory of Arable Land Conservation in North China, Ministry of Agriculture and Rural Affairs, Beijing 100193, China.
E-mail addresses: wjmeng200702@163.com (W. Meng), xjl1263780481@163.com (J. Xing), 15955701818@163.com (M. Niu), qiangzuo@cau.edu.cn (Q. Zuo), wuxun@cau.edu.cn (X. Wu), shijianchu@cau.edu.cn (J. Shi), sjd@xjau.edu.cn (J. Sheng), jpa@xjau.edu.cn (P. Jiang), chqjia@126.com (Q. Chen), bengal@volcani.agri.gov.il (A. Ben-Gal).

https://doi.org/10.1016/j.agwat.2022.107994
Received 8 August 2022; Received in revised form 6 October 2022; Accepted 25 October 2022
Available online 1 November 2022

delivered as fertigation products. During the fertigating process, nutrients are carried by infiltrating water flow and transported downwards rapidly, with the downward transport subsequently declining and ultimately ceasing (Hanson et al., 2006; Azad et al., 2018). Consequently, the earlier fertilizer is applied during an irrigation event, the deeper nutrients are transported. Formulation of a fertigation protocol including rate and timing of injection and delivery of nutrients is critical for efficient fertilizer use, but is closely related to nutrient types, soil water flow conditions, root distribution and initial soil nutrient status (Russo, 2016; Kim et al., 2018; Chen et al., 2019). There has been quite some speculation regarding design of such protocols but there is little data- and/or mechanism-based evidence regarding optimal fertilizer application schemes in fertigation systems (Silber et al., 2003; Bar-Tal et al., 2020).

Due to the simplicity of its operation, the single-pulse application method (SPAM), in which fertilizer is injected and delivered in a single dose, alternatively in the early, middle or late stage of an irrigation event, has been widely adopted (Cote et al., 2003; Hou et al., 2007, 2009). Generally, SPAM tends to create zones of nutrient accumulation. With the backward adjustment of fertilizer application timing from early to middle and even to late stage, nutrient accumulation zone gradually moves up from deeper to upper soil layers (Azad et al., 2018; Ma et al., 2021). Experimental studies indicated that late-stage SPAM was more efficient in enhancing crop yield and fertilizer use efficiency (Hou et al., 2007). However, inconsistent experimental results were subsequently found by the same research team, with similar or even decreased yield driven by late-SPAM (Hou et al., 2009). Contradictory results simulated with the HYDRUS-2D model (Simunek et al., 1999) were also provided by Cote et al. (2003) and Gärdenäs et al. (2005), according to different assumptions and parameters regarding root distribution and uptake, as well as other simulation conditions. Therefore, we suggest that optimal and efficient fertigation schemes should be based on the processes and mechanisms affecting nutrient transport and uptake.

Besides the amount of nutrients in root zone, root nutrient uptake is also undoubtedly influenced by nutrient distribution relative to roots. In cases with constant soil nutrient amount and identical water and salinity conditions, consistent distribution patterns, implying more nutrients in soil layers with more roots, should be beneficial for nutrient uptake due to shorter distance and lower resistance for nutrient transport from soil to roots. Otherwise, if the majority of nutrients are located in soil layers with few roots, the longer distance and higher resistance of nutrient transport to roots will complicate uptake (Goins and Russelle, 1996; Schwab et al., 2000). Crop roots are typically distributed in shallow soil layers and gradually lessen with soil depth (Zuo et al., 2013; Ning et al., 2015, 2019). This likely explains why late-stage SPAM has been found more favorable to crop nutrient uptake than early- or middle-stage SPAM, representing a higher coincidence degree between nutrients and roots.

Hence, we hypothesized that enhancing the coincidence degree between nutrients and roots would be an effective way to promote nutrient uptake and thus increase fertilizer use efficiency. Subsequently, the objective of this study was to improve fertigation scheduling by injecting and delivering fertilizer according to root distribution and comparing its performance with the traditional approaches. Xinjiang is a typical arid region in China with an important agriculturally based economy. We took the most popular crop in this region, drip-irrigated cotton under film mulch, as a case study to evaluate and optimize fertigation protocols. A two-year field experiment was conducted to explore the effects of various fertilizer application scenarios on nutrient (soil mineral N, available P and K) transport and uptake.

2. Materials and methods

2.1. Improving fertigation protocols based on root distribution

Crop root density typically demonstrate a decreasing trend from soil surface to rooting depth. Although root distributions are strongly dependent on the interactive effects of crop species, growth stages, soil and climate conditions, irrigation and fertilization, the distributions of normalized root length density (NRLD) can often be described by a generalized function as follows (Zuo et al., 2013):

$$L_{nrd}(z_r) = p(1 - z_r)^{p-1} \quad (1)$$

where z_r is the normalized soil depth ranging from 0 at soil surface to 1 at rooting depth, $z_r = z/L_r$, z is the vertical coordinate originating from soil surface and positive downward (cm), and L_r is rooting depth (cm); $L_{nrd}(z_r)$ is NRLD, representing the ratio of root length density at z_r to the average over root zone; p is a fitting parameter, representing the NRLD at the soil surface, mainly dominated by crop's genetic characteristics and independent of other environmental factors, and recommended as 1.96 for cotton (Fig. 1) by Ning et al. (2015). Therefore, the generalized function, established and tested by a large amount of measured NRLD data (Zuo et al., 2013; Ning et al., 2015), was adopted to propose a root distribution-based multistage application method (RMAM) for scheduling fertilizer injection and delivery during the fertigating process.

To match root distribution, different percentages of fertilizer were applied at different relative times during each irrigation event. The following steps were universally proposed to optimize fertilizer application according to root distribution:

(1) Divide an irrigation event into n stages evenly from beginning to end, and additionally divide the root zone into n layers from rooting depth to soil surface, with the i^{th} stage corresponding to the i^{th} layer ($i = 1, 2, \ldots, n$);
(2) Calculate the proportion of roots in each soil layer to those in the whole root zone according to the function of NRLD;
(3) Set the proportion of roots in the i^{th} layer calculated in step (2) as the proportion of fertilizer applied in the i^{th} stage ($i = 1, 2, \ldots, n$), and then calculate the amount of fertilizer delivered within each stage.

Theoretically, larger n means higher coincidence degree between soil nutrients and roots, and infinite n leads to continuous injection. From a practical point of view, each irrigation process was evenly divided into early, middle and late stages ($n = 3$) as an example in this study, and correspondingly, deep, intermediate and shallow layers were set in the root zone. The NRLD profile of cotton (Fig. 1) indicated that the proportions of roots were 11%, 32% and 57%, respectively, for the deep, intermediate and shallow layers, which were then reflected in the

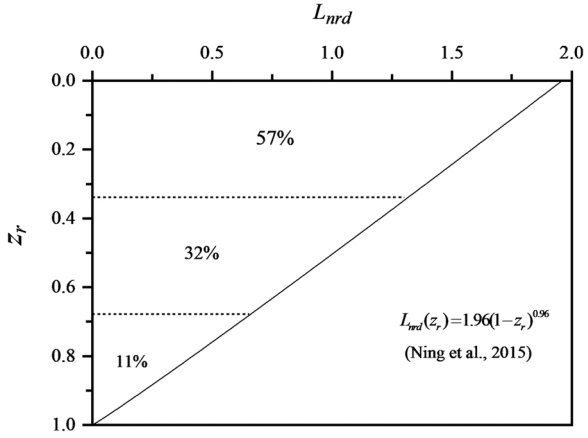

Fig. 1. The generlized profile of normalized root length density for cotton (L_{nrd}) along the normalized soil depth (z_r) in Ning et al. (2015). The percentages (11%, 32% and 57%) represent the proportions of roots in the deep ($1 \geq z_r > 0.67$), intermediate ($0.67 \geq z_r \geq 0.33$) and shallow layers ($0.33 > z_r \geq 0$) of root zone, respectively.

relative rates of fertilizer application in the early, middle and late stages of each irrigation event.

2.2. Field experiment

The experimental site was located in the cotton breeding base of Xinjiang Agricultural University (85° 40′ 33″ E, 44° 26′ 20″ N, altitude 490 m), Shawan county, Xinjiang, China (Liu et al., 2022). The station is in a continental temperate arid region with annual values of 6.3–6.9 °C mean temperature, 170–190 d frost-free period, 140–350 mm precipitation, and 1500–2000 mm evaporation. The soil from 0 to 100 cm can be divided into three layers with an average salt content of 4.19 g kg^{-1} (Table 1). Soil water retention was measured with a pressure membrane plate (Soil Moisture Equipment Co., USA) and described with the closed form of van Genuchten (1980). Field water capacity was determined as the soil water content corresponding to − 300 cm soil matric potential for silty loam (Romano and Santini, 2002). In order to maintain normal cotton growth in this region, supplementary irrigation is essential, and irrigation water was therefore taken from a nearby well with a salt content of 0.49 g L^{-1}, a pH value of 7.85 and an electrical conductivity of 932.65 μS cm^{-1}. An automatic agro-meteorological station (WeatherHawk 500, Campbell Scientific, USA) was installed to monitor climate data including air temperature, relative humidity, rainfall, solar radiation, and wind speed.

A field experiment was carried out over two years. With initial water storages of 214.58 and 196.26 mm in 0–100 cm soil layer, cotton (*Gossypium hirsutum* L., Xinnongda 4) was sowed in 12 and 20 independent plots on 21 and 18 April in 2019 and 2020, and harvested on 28 (160 days after sowing: 160 DAS) and 22 September (157 DAS), respectively. Each plot (690 cm wide by 750 cm long) contained three strips with a planting mode of "one film, three tapes and six rows" (Fig. 2A). The interval between plants was 12 cm in each row, and the space between emitters (2.4 L h^{-1}) was 30 cm along the drip tape. During the two growing seasons, irrigation was scheduled according to the local practice. In 2019, 318.38 mm water was applied over nine events, and 330.00 mm was applied in 2020 over 10 events (Table 2). In each growing season, the first irrigation event was designed for germination within several days after sowing without fertilizer application, and the remaining irrigation events were synchronized by fertilization. Irrigation was delayed in case of rain, and the total precipitation during the growing seasons was 147.90 mm in 2019 and 63.20 mm in 2020 (Table 2). The specific amount of fertilizer was determined according to the expected nutrient demand at each growth stage of cotton. The fertilizer allocation percentages in seedling, budding, flowering-boll, and boll-opening stages were set as 3%, 23%, 67%, and 7%, respectively, according to the nutrient demand along various growth stages and dry matter accumulation pattern (Makhdum et al., 2007; Liu et al., 2022). Urea, monoammonium phosphate and potassium sulfate were applied as N-P_2O_5-K_2O at a rate of 187.01–139.65–130.05 kg ha^{-1} in 2019 and 187.01–97.77–91.03 kg ha^{-1} in 2020. In 2019, P and K were consistent with the local practice, while N in 2019 and all nutrients in 2020 were only 70% of the local application. Each irrigation process was evenly divided into three stages, and four (T1-T4) and five (T1-T5) fertigation application treatments were evaluated in 2019 and 2020 with three and four replicates, respectively (Fig. 2B). The treatments of T1, T2 and T3 represented early-, middle- and late-stage SPAM. For T4 treatment, RMAM was applied with the corresponding percentages of 11%, 32% and 57%, respectively. A uniform multistage application method (UMAM) was referenced as T5 treatment in 2020, delivering fertilizer evenly in the early, middle, and late stages. Field management measures such as topping, herbicide and insecticide were conducted according to local commercial practices (Chen et al., 2010; Zong et al., 2021).

To investigate the effects of fertilizer application protocols on soil water and nutrient dynamics, 3–4 soil sampling events were carried out within a typical fertigation period in the late flowering-boll stage with strong demand for water and nutrient. In 2019, periodic soil sampling started on 109 DAS prior to the fertigation event on 110 DAS and followed by two sampling events on 111 and 116 DAS before the next fertigation event on 118 DAS. Similarly, the periodic soil sampling in 2020 started on 89 DAS before the fertigation event on 90 DAS, and then three sampling events were conducted on 91, 93, 98 DAS, but the following fertigation event designed on 99 DAS was actually carried out on 104 DAS due to rainfall. Around a cotton seedling randomly chosen from the bilateral strips in each plot, an auger (8 cm inner diameter and 20 cm length) was used to sample soil at a 10 cm vertical interval from 5 to 95 cm (Fig. 2A), and rooting depth was determined when few roots were found in deeper soil. In order to investigate the effects of fertilizer application protocols on cotton growth, as well as soil water and nutrient reserves, three additional crop and soil sampling events were also implemented in the early and late flowering-boll stages prior to fertigation and in the late boll-opening stage before defoliant spraying and harvest (79, 99 and 147 DAS in 2019; 83, 103 and 144 DAS in 2020). For each sampling, three plants were randomly selected from the bilateral strips in each plot to obtain the canopies. Around one of the three plants, soil was sampled as the same way mentioned above, and rooting depth was also monitored.

Each soil sample was divided into four parts to measure the contents of water, mineral N (NO_3^--N and NH_4^+-N), available P and K, respectively, through the methods as follows (Tao et al., 2017; Wang et al., 2021; Zong et al., 2021). The first part was dried to constant weight at 105 °C for soil water content. The second was extracted with 2.0 mol L^{-1} KCl as a ratio of 1:5, and mineral N was analyzed by a flow auto-analyzer (AA3, SEAL Analytical, Germany). The third was air-dried and extracted with 0.5 mol L^{-1} $NaHCO_3$ as a ratio of 1:20, and available P was analyzed by a flow auto-analyzer. The fourth was also air-dried but extracted with 1.0 mol L^{-1} NH_4OAc as a ratio of 1:20, and available K was analyzed by an atomic absorption spectrophotometer (PinAAcle 900 T, PerkinElmer, USA). The sampled leaves were scanned and then analyzed by the WinRHIZO Pro software package (Regent Instruments Inc., Quebec, Canada) for leaf area. Dry weight of canopy was obtained by drying to constant weight at 75 °C. Mineralized with H_2SO_4 and H_2O_2, N and P in aboveground biomass were analyzed by a flow auto-analyzer, and K was measured by an atomic absorption spectrophotometer. By excluding 1.5 m at both ends of the middle strip, a non-sampling zone (4.5 × 2.3 m^2) was reserved to measure yield manually.

2.3. Calculation of indexes

Fertilizer partial productivity (*PFP*, kg kg^{-1}) was estimated as (Yang et al., 2014; Liang and Shi, 2021):

Table 1
Soil properties in the experimental field: contents of sand, silt, and clay particles, soil bulk density (ρ_b), saturated water content (θ_s), residual water content (θ_r), field water capacity (θ_f), saturated hydraulic conductivity (K_s), and the fitting parameters in van Genuchten's (1980) soil water retention curve (α and n).

Depth (cm)	Sand (%)	Silt (%)	Clay (%)	ρ_b (g cm^{-3})	K_s (cm d^{-1})	θ_s (cm^3 cm^{-3})	θ_r (cm^3 cm^{-3})	θ_f (cm^3 cm^{-3})	α (cm^{-1})	n
0–30	22.73	53.45	23.82	1.44	7.76	0.44	0.05	0.22	0.05	1.31
30–60	18.52	60.89	20.59	1.63	1.69	0.39	0.06	0.20	0.06	1.30
60–100	23.11	56.64	20.25	1.46	4.22	0.42	0.03	0.22	0.06	1.24

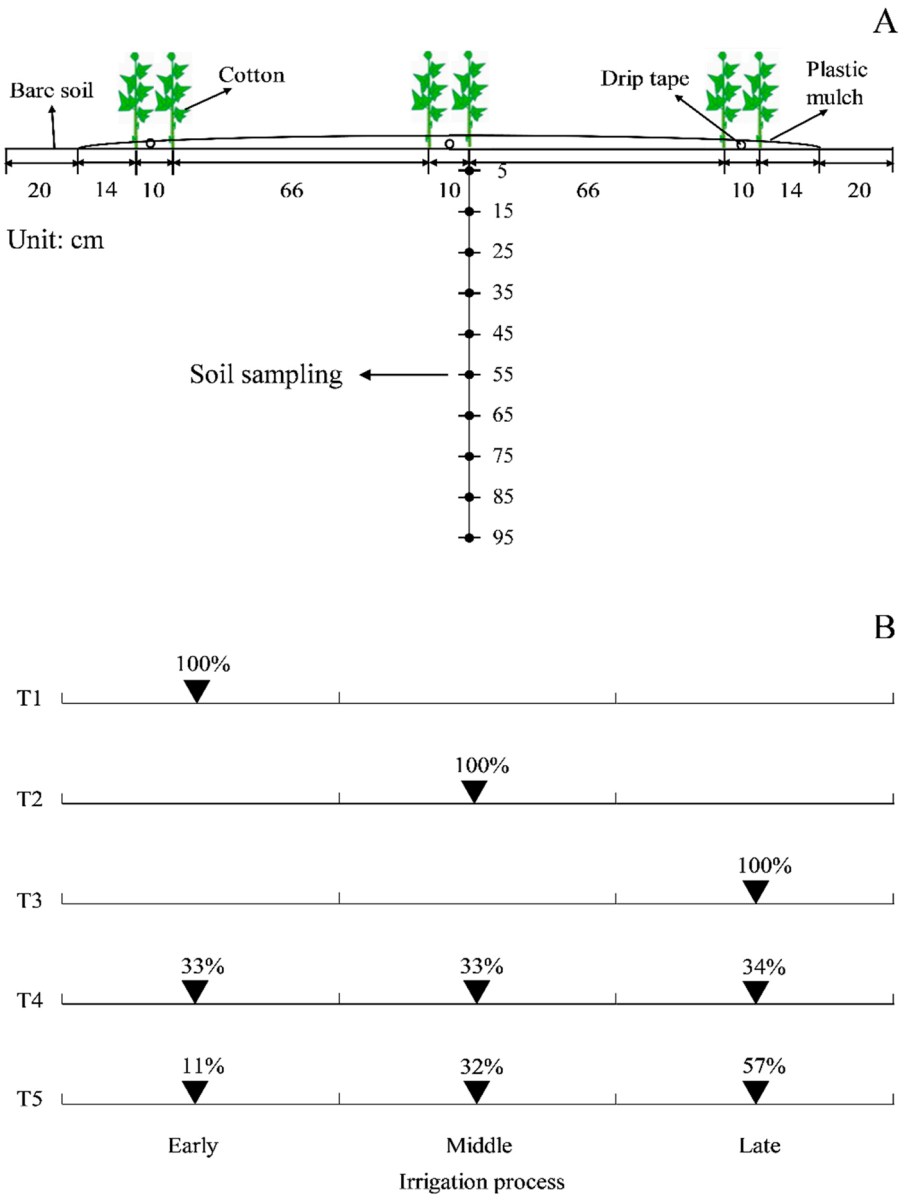

Fig. 2. Schematic diagram of planting-drip irrigation mode and soil sampling for a typical strip (A) and fertilizer application schemes of T1-T5 treatments (B). The percentages represent the fertilizer injection proportions in the early, middle and late stages of an irrigation event.

Table 2
The rainfall and the schemes of irrigation and fertilization in the growing seasons of 2019 and 2020. The rainfall represents the accumulation during each period. DAS represents days after sowing.

2019						**2020**					
DAS	Rainfall (mm)	Irrigation (mm)	Fertilizer (kg ha^{-1})			DAS	Rainfall (mm)	Irrigation (mm)	Fertilizer (kg ha^{-1})		
			N	P_2O_5	K_2O				N	P_2O_5	K_2O
3	10.10	37.50	–	–	–	6	0.00	60.00	–	–	–
62	93.50	35.11	38.51	28.76	26.78	55	12.30	30.00	33.92	17.73	16.51
70	0.10	35.11	13.77	10.28	9.57	61	0.40	30.00	9.18	4.80	4.47
80	10.80	35.11	22.95	17.14	15.96	75	17.80	30.00	29.83	15.60	14.52
90	0.00	35.11	22.95	17.14	15.96	84	5.30	30.00	20.66	10.80	10.06
100	13.60	35.11	22.95	17.14	15.96	90	0.20	30.00	13.77	7.20	6.70
110	0.00	35.11	20.66	15.42	14.36	104	12.30	30.00	32.13	16.80	15.64
118	7.70	35.11	18.36	13.71	12.77	110	1.20	30.00	13.77	7.20	6.70
127	2.40	35.11	26.86	20.06	18.68	115	0.00	30.00	11.48	6.00	5.59
160	9.70	–	–	–	–	120	1.00	30.00	22.27	11.64	10.84
						160	12.70	–	–	–	–
Sum	143.90	318.38	187.01	139.65	130.05	Sum	63.20	330.00	187.01	97.77	91.03

$$PFP = Y/F \quad (2)$$

where Y was cotton yield (kg ha^{-1}); F was the corresponding application rate of N, P_2O_5 or K_2O during growth season, respectively (kg ha^{-1}).

During the typical fertigation period, soil water flux through the lower boundary of root zone (q_w, mm d^{-1}) was calculated according to Darcy's law (Chen and Liu, 2002; Wang et al., 2006):

$$q_w = -10K(h)\left(\frac{\partial h}{\partial z} - 1\right) \quad (3)$$

where h was the soil matric potential at the lower boundary of root zone (cm), determined according to the measured soil water content and the soil water retention curve; $K(h)$ was the soil hydraulic conductivity (cm d^{-1}). Subsequently, soil nutrient flux (q_n, kg ha^{-1} d^{-1}) was estimated as:

$$q_n = 0.01 q_w C_s \quad (4)$$

where C_s was the concentration of nutrient in soil solution (mg L^{-1}).

To compare the distribution patterns between soil nutrients and roots under each treatment, soil nutrient contents, measured at a 10 cm interval in root zone during the typical fertigation period, were normalized as the function initially proposed for root length density (Wu et al., 1999):

$$C_n(z_r) = \frac{C(z_r)}{\int_0^1 C(z_r)dz_r} \quad (5)$$

where $C_n(z_r)$ was the normalized soil nutrient content, representing the ratio of nutrient content at z_r to the average in root zone; $C(z_r)$ was soil nutrient content (mg kg^{-1}). To quantitatively evaluate the coincidence degree between the normalized profiles of soil nutrient content and root length density, three indicators such as correlation coefficient (R), coefficient of determination (R^2) and residual sum of squares (R_{SS}) were adopted.

2.4. Statistical Analysis

All experimental data were shown as the averages of replicates and analyzed by Microsoft Excel 2019 (Microsoft Corporation, USA). Origin software (Origin Lab , USA) was used to plot figures. SPSS 20.0 software package (International Business Machines Corporation, USA) was applied to conduct the analysis of variance (ANOVA). A Duncan multiple range test at $P < 0.05$ was carried out to determine if significant difference occurred among treatments.

3. Results

3.1. The effects of fertigation protocols on soil water and nutrient dynamics

The field experimental data in 2019 and 2020 indicated that fertilizer application schemes did not significantly affect soil water dynamics. For any soil sampling event, no significant difference was found among the treatments for the average soil water contents in 0–100 cm ($P < 0.05$), and the standard error of soil water contents at each depth was generally less than 0.05 cm^3 cm^{-3}. Therefore, for each sampling event, the soil water contents measured at same depth were averaged under all the treatments with 12 replicates in 2019 and 20 replicates in 2020 (Fig. 3). Within the typical fertigation periods (2019: 109–118 DAS; 2020: 89–104 DAS), soil water contents in the bottom zone from 60 to 100 cm were hardly impacted by irrigation and root water uptake, and tended to be constant at 0.20 ± 0.05 cm^3 cm^{-3}, corresponding to about 90% of field water capacity (Fig. 3). Nevertheless, in the middle (30–60 cm) and especially top (0–30 cm) zones, soil water contents changed drastically, rapidly increasing after irrigation (111 DAS 2019 and 91 DAS in 2020) and then gradually decreasing until the next irrigation event. Rooting depth reached 80 cm at the early flowering-boll stage (about 80 DAS) and remained unchanged until harvest. Mainly driven by the gravitational potential gradient, the relatively stable soil water contents at 60–100 cm led to deep leaching through the lower boundary of root zone. The total leachates during the typical sampling periods of 109–116 DAS in 2019 and 89–98 DAS in 2020 were 0.94 and 1.30 mm, respectively. Daily leaching beyond the root zone increased to a maximum on the 3rd day after fertigation (e.g., 0.18 mm d^{-1} on 93 DAS in 2020), and subsequently decreased until the next irrigation event (Fig. 4A).

Compared to soil water, soil nutrient dynamics was more complicated, influenced by fertilizer application schemes and nutrient type (Figs. 4B and 5). The effects in the two growing seasons were fairly consistent, and thus only the soil nutrient dynamics during the typical fertigation period in 2020 is presented (Fig. 5), including all the designed fertigation protocols (T1-T5) and the considered nutrients (soil mineral N, available P and K). Due to the slow decomposition process of

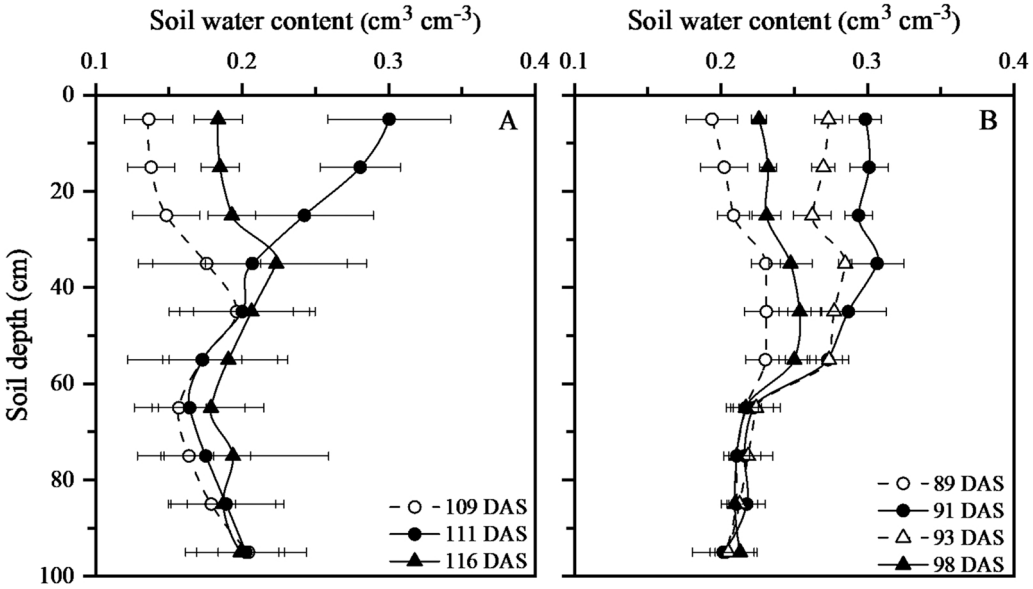

Fig. 3. The soil water dynamics from soil surface to 100 cm depth for various treatments during 109–116 DAS in 2019 (A) and during 89–98 DAS in 2020 (B). Error bars indicate standard errors, and DAS represents days after sowing.

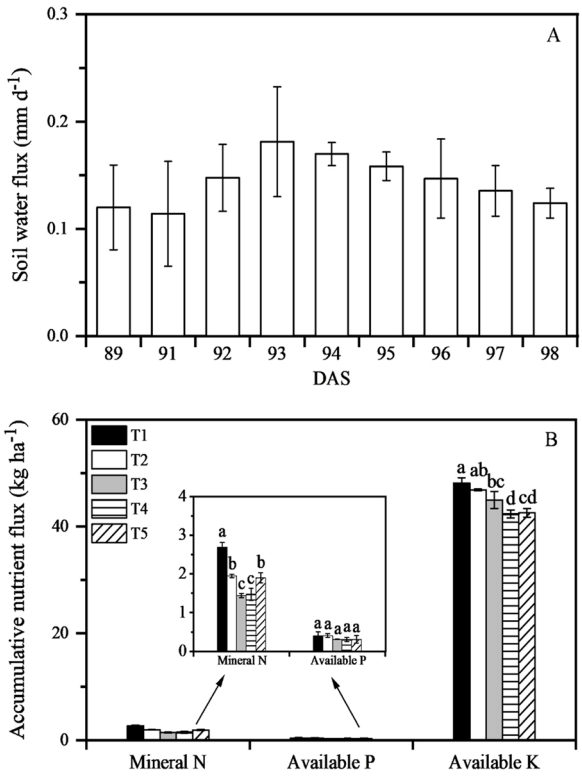

Fig. 4. The daily soil water flux (A) and the accumulative flux of soil mineral N, available P and K (B) through the lower boundary of root zone under various fertilizer application treatments (T1-T5) in 2020 (89–98 DAS). Error bars indicate standard errors, and DAS represents days after sowing.

urea, on the 1st day after fertigation (91 DAS), soil mineral N (NO_3^--N and NH_4^+-N) content at any depth was only a little higher than that prior to fertigation on 89 DAS, while N significantly increased to a maximum content on the 3rd day (93 DAS). Thereafter on the 8th day (98 DAS), soil mineral N content in each soil layer fell back to close to initial level before fertigation (Fig. 5A). The profiles on 93 DAS fully demonstrated the differences among treatments, especially N accumulation due to SPAM. Postponing fertilizer application time from the early stage of an irrigation event (T1) to middle (T2) or even late stage (T3), N accumulation shifted from the bottom to middle or even to top zone. Whether for the early-, middle- or late-stage SPAM, the average soil mineral N content in the accumulation zone (about 30 cm in depth) reached nearly twice that found in the other soil layers. Different from T1 and T2, soil mineral N contents under T3 generally decreased with soil depth, like the generalized distribution of NRLD (Fig. 1). Under the T4 treatment (RMAM), soil mineral N contents also gradually decreased with soil depth in a pattern similar to NRLD. Compared to late-stage SPAM, RMAM led to lower soil mineral N content in the top zone and higher content in the bottom zone (Fig. 5A). In comparison to SPAM and RMAM, uniform application in the early, middle and late stages (UMAM, T5) caused a more homogeneous profile of soil mineral N content with no observed accumulation. Under T2 and especially T1 treatments, soil mineral N content was negatively related to NRLD (Table 3). Compared to T1, T2 and T5 treatments, between the normalized profiles of root length density and soil mineral N content on 93 DAS, higher correlation coefficient (R) and determination coefficient (R^2) and lower residual sum of squares (R_{SS}) were found under T3 and especially T4 treatments (Table 3).

Different from soil mineral N, available P and K at almost every depth reached the maximal content on the 1st day after fertigation (91 DAS), and then gradually fell back to the similar level prior to fertigation until the next fertigation event (Fig. 5B and C). In general, fertilizer application protocols influenced soil available P and K dynamics in similar patterns as soil mineral N, but the effects on available K were weaker and even less on available P. Between the normalized profiles of root length density and soil available P and K contents on 91 DAS, the highest R and R^2 were also observed under T4, and the lowest R_{SS} occurred under T3 or T4. Relative to soil mineral N and available K, most available P tended to accumulate in the upper soil layers in a similar manner, and thus the difference of R, R^2 and R_{SS} among the five treatments was smaller (Fig. 5B, Table 3). However, compared to the early-, middle- or late-stage SPAM, the multistage application methods (RMAM and UMAM) resulted in available P distributions more similar to NRLD with higher R and R^2, as well as lower R_{SS}.

With deep leaching of soil water (Fig. 4A), nutrient leaching through the lower boundary of the root zone occurred regardless of fertigation protocols (Fig. 4B). Although the loss of soil available P by leaching was small and nearly negligible, it was significant for mineral N and especially available K. During the typical fertigation periods for all the treatments, the average leachates of mineral N and available P and K were 1.13, 0.58 and 42.98 kg ha^{-1} in 2019, and 1.89, 0.34 and 44.96 kg ha^{-1} in 2020, respectively. The leaching loss of available P was not significantly affected by fertilizer application schemes. For mineral N or available K, leachate loss was always the highest when fertilizer was applied in the early stage (T1) and decreased gradually when application was postponed to middle (T2) and to late (T3) stages. Compared to late-stage SPAM, the deep losses under UMAM were higher and similar under RMAM for mineral N, but both lower for available K (Fig. 4B). The data in both years, measured before fertigation and harvest, indicated that the temporary effects of fertilizer application schemes on soil nutrient dynamics (Fig. 5) led to cumulative effects on soil nutrient reserves (Fig. 6). Compared to early-, middle-stage SPAM or UMAM, late-stage SPAM and especially RMAM resulted in lower soil nutrient (especially mineral N) reserves in 0–100 cm (especially 60–100 cm).

3.2. *The effects of fertigation protocols on cotton growth and nutrient uptake*

Compared to 2019, even with identical fertilizer application schemes, growth indicators and yield in 2020 were lower with less rainfall and application of P and K fertilizers (Table 2). Cotton under the different fertilizer application treatments maintained a relatively uniform growth pattern in the two growth seasons. Leaf area decreased slowly after reaching a maximum at the late flowering-boll stage (about 100 DAS), while aboveground dry weight increased continuously (Fig. 7). However, plant growth dynamics were affected following three fertilizer application events with different schemes (e.g., on 83 DAS in 2020). Significant differences in leaf area index and aboveground dry weight were maintained until harvest (Fig. 7) and were finally reflected in cotton yield (Fig. 8A).

When other conditions were the same for the three treatments of SPAM, changing fertilizer application timing from early stage of an irrigation event (T1) to middle (T2) and further to later stage (T3) led to a general increasing trend for cotton growth indexes such as leaf area index and aboveground dry weight (Fig. 7), as well as yield and nutrient use efficiency (Fig. 8). However, the effects were not always obvious, and almost all significant increases occurred after the late flowering-boll stage. Compared to T1 and T2, for example, significant enhancement in cotton growth under T3 was found after 100 DAS in both 2019 and 2020, while yield was only significantly affected in 2020 with an increase of 5.7–6.8%. Resulting from the backward adjustment of fertilizer injection timing, the positive effects on cotton growth and production under T3 were supported by more root nutrient uptake (Fig. 9). The experimental results in 2020 showed that, compared to UMAM (T5), although late-stage SPAM (T3) failed to enhance yield and nutrient use efficiency (Fig. 8), while cotton growth and nutrient uptake (Figs. 7 and 9) were significantly promoted. Additionally, compared to T3, RMAM

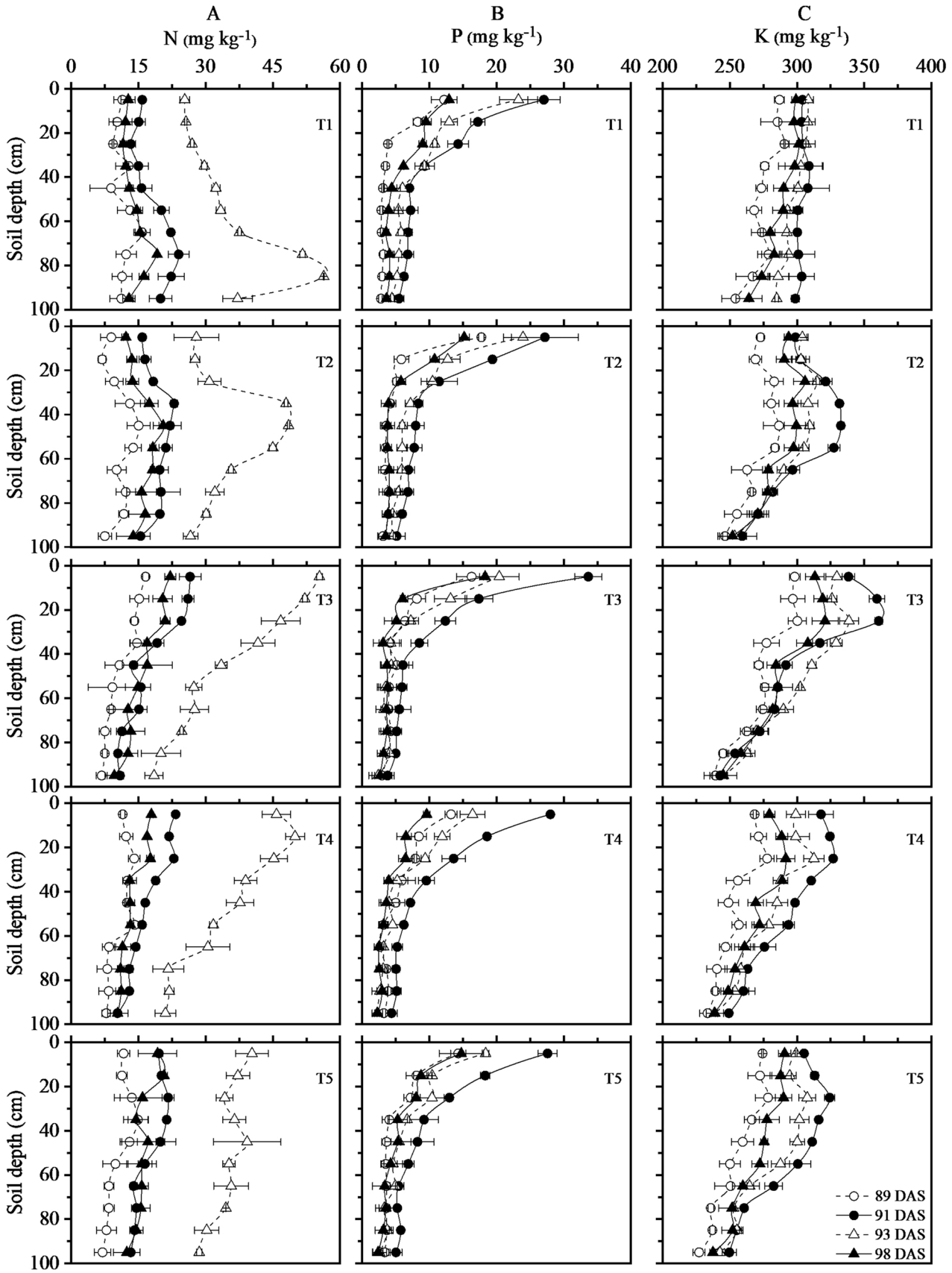

Fig. 5. The dynamics of soil mineral N (A), available P (B) and K (C) from soil surface to 100 cm depth under various fertilizer application treatments (T1-T5) in 2020 (89–98 DAS). Error bars indicate standard errors, and DAS represents days after sowing.

Table 3
The correlation coefficient (R), coefficient of determination (R^2) and residual sum of squares (R_{SS}) between the normalized profiles of soil nutrient content and root length density during the fertigation period (89–98 DAS) in 2020 for the five fertilizer application treatments (T1-T5). DAS represents days after sowing.

DAS	Soil nutrients	R					R^2					R_{ss}				
		T1	T2	T3	T4	T5	T1	T2	T3	T4	T5	T1	T2	T3	T4	T5
93	Mineral N	-0.90	-0.36	0.95	0.96	0.56	0.80	0.13	0.89	0.92	0.32	5.13	3.77	0.94	1.07	2.39
91	Available P	0.87	0.85	0.85	0.90	0.90	0.75	0.72	0.71	0.81	0.81	0.80	0.97	1.28	0.65	0.72
91	Available K	0.89	0.18	0.90	0.93	0.77	0.79	0.03	0.80	0.86	0.59	2.44	2.58	1.88	2.11	2.24

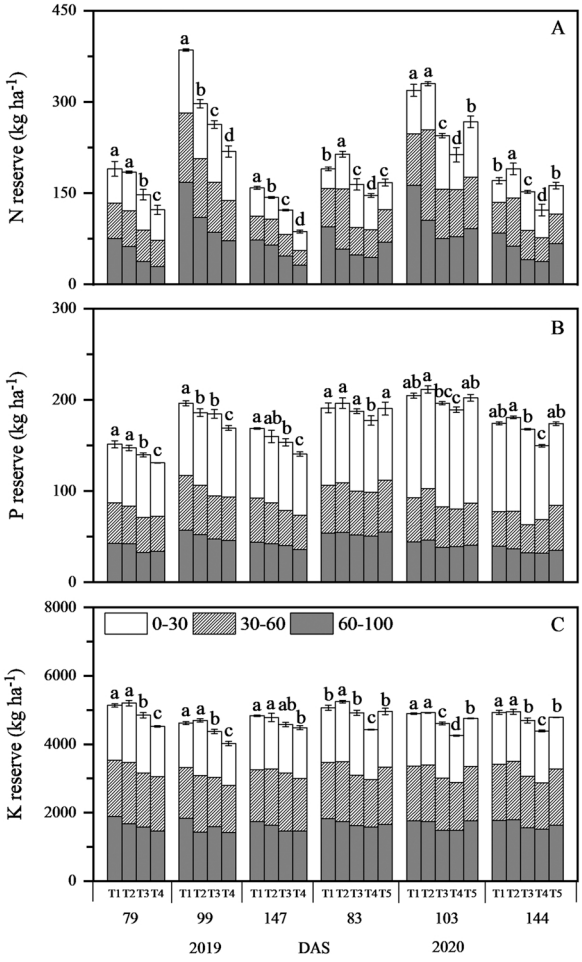

Fig. 6. The dynamic reserves of soil mineral N (A), available P (B) and available K (C) in 0–30, 30–60 and 60–100 cm under various fertilizer application treatments (T1-T5) in 2019 and 2020. Different lowercase letters indicate significant difference in 0–100 cm soil nutrient reserves among treatments ($p < 0.05$). Error bars indicate standard errors, and DAS represents days after sowing.

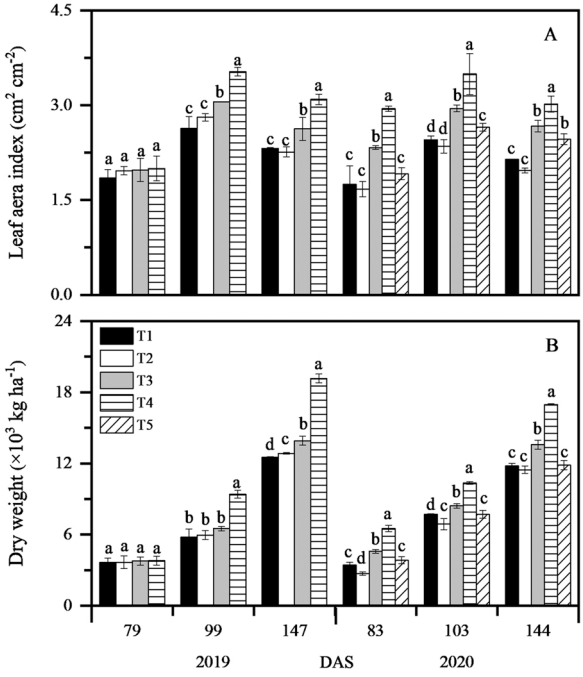

Fig. 7. Leaf area index (A) and aboveground dry weight (B) at various growth stages of cotton under fertilizer application treatments (T1-T5) in 2019 and 2020. Different lowercase letters in the same growth period indicate significant difference among treatments ($p < 0.05$). Error bars indicate standard errors, and DAS represents days after sowing.

(T4) significantly facilitated nutrient uptake and plant growth with an increased range higher than 10% for the corresponding indexes in the late boll-opening stage (Figs. 7 and 9). Driven by RMAM, the increase in cotton yield reached 4.9% in 2020 and 6.2% in 2019, leading to an average increase of 5.5% in fertilizer partial productivity (Fig. 8). Obviously, among the five fertilizer application schemes, RMAM was the optimal leading to the highest yield and fertilizer use efficiency.

4. Discussion

Fertigation scheduling during drip irrigation events did not significantly affect soil water dynamics during both experimental seasons. Based on the local irrigation experience, the profile averaged soil water contents were kept almost higher than 70% of field water capacity for all treatments (Fig. 3), within an optimal soil water range (Feddes et al., 1978), leading to desired growth and yield of cotton at the cost of significant deep leaching losses of water and nutrients (Fig. 4). Besides nutrient types, nutrient leaching loss was also strongly dependent on fertilizer application schemes (Fig. 4B). Under the optimal soil water conditions (Fig. 3), fertilizer application schemes significantly influenced soil nutrient dynamics (Fig. 5) by dominating the duration and distance of convection transport of solutes carried by downward soil water flow. Even for nearly stable soil water contents below 60 cm depth, the existing gravitational potential gradient drove soil nutrients to the depth of 60–80 cm or even beyond the rooting depth of 80 cm. Theoretically, the earlier fertilizer is applied during an irrigation event, the deeper nutrients will be transported (Azad et al., 2018 and 2020), but this effect is also dependent on solute mobility (Donagemma et al., 2008; Brown et al., 2017). For mobile ions such as mineral N and available K, early-, middle- and late-SPAM readily caused nutrient accumulation in the bottom (60–100 cm), middle (30–60 cm) and top zone (0–30 cm), respectively (Fig. 5), agreeing well with the previous studies (Ma et al., 2021). Therefore, relative to late-SPAM with identical water leaching (Fig. 4A), middle- especially early-SPAM resulted in more nutrient leaching loss (Fig. 4B), which was proportional to the nutrient concentration in soil solution advected across the lower boundary of the root zone as Eq. (4). Different from mineral N and available K, available P is more difficult to mobilize and transport, and

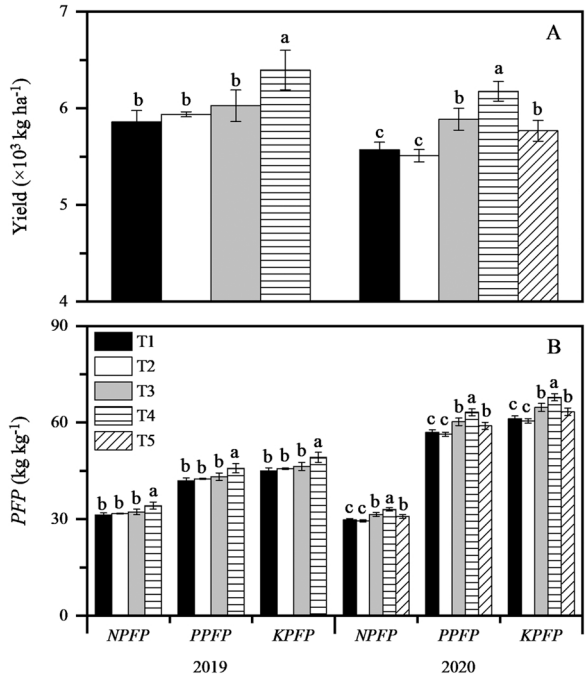

Fig. 8. Cotton yield (A) and fertilizer partial productivity (*PFP*) for N, P and K (*NPFP*, *PPFP* and *KPFP*) (B) under various fertilizer application treatments (T1-T5) in 2019 and 2020. Different lowercase letters indicate significant difference among treatments ($p < 0.05$). Error bars represent standard errors.

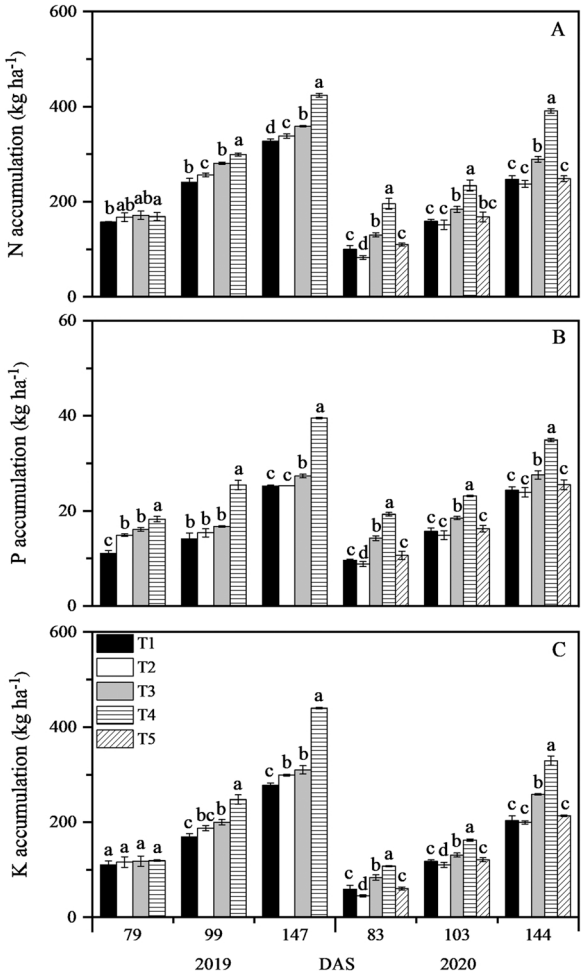

Fig. 9. Aboveground accumulation of N (A), P (B) and K (C) at various growth stages of cotton under various fertilizer application treatments (T1-T5) in 2019 and 2020. Different lowercase letters in the same growth period indicate significant difference among treatments ($p < 0.05$). Error bars indicate standard error, and DAS represents days after sowing.

thus most of the P was concentrated in the upper soil layers for all the three SPAM treatments. However, middle- and especially early-SPAM relieved the accumulation effect and transported more available P to deeper soil layers (Fig. 5B). Adjusting pulse application from one (SPAM) to three times (RMAM and UMAM), nutrient accumulation was avoided to some extent for mineral N and available K, and for available P, it was also significantly mitigated as a result of higher fertilizer application frequency (Clothier and Green, 1994; Ben-Gal and Dudley, 2003; Mohammad et al., 2004). Among the five schemes, RMAM minimized deep nutrient leaching due to the lowest soil nutrient content at the lower boundary of root zone. A smoother and more favorable soil nutrient profile might be expected by increasing fertilizer application frequency or even carrying out a continuous application scheme based on RMAM.

For early-stage SPAM, the lowest coincidence degree between the normalized profiles of soil nutrient content and root length density (Table 3) was related to inconsistent or even opposite distributions (Figs. 1 and 5), which would cause the greatest resistance for root uptake (Goins and Russelle, 1996; Schwab et al., 2000). Taking the situation on 93 DAS (the 3rd day after fertigation) in 2020 as an example, the roots in the shallow layer (0–27 cm) of root zone (0–80 cm) accounted for 57% (Fig. 1) but were surrounded by only 28% of the total root zone mineral N under the T1 treatment. Relative to root uptake demand, insufficient N supply in this soil layer led to the lowest average soil mineral N content on 98 DAS (12.5 mg kg^{-1}) among the five treatments (Fig. 5A). In contrary, for the deep layer (53–80 cm) of root zone, 11% of roots were supplied by 41% of the total mineral N, and thus surplus N exceeding root uptake demand was readily percolated downward (Fig. 4B). Therefore, among the five schemes, early-stage SPAM resulted in the lowest nutrient uptake (Fig. 9) and highest leaking loss (Fig. 4B) and soil reserve (Fig. 6), as well as the minimum growth indices (Fig. 7), yield and fertilizer use efficiency (Fig. 8). Since more nutrients, especially available P, were accumulated in the shallow layer and less in the middle and deep layers of root zone, coinciding better with roots, late-SPAM obtained better results than middle- and especially early-SPAM in many aspects such as deep leaking, soil residual, root uptake, crop growth and yield (Figs. 4–9, Table 3). This finding was generally consistent with previous studies, indicating that the widely adopted late-SPAM is generally reasonable (Hou et al., 2007; Azad et al., 2018; Ma et al., 2021). In a two-year greenhouse experiment conducted by Hou et al. (2007), compared to early-SPAM, late-SPAM increased cotton yield by 12.1%. However, a field experiment (Hou et al., 2009) showed a slight decrease of cotton yield for late-SPAM under conditions of moderate salinity, but no differences were found under low or high salinity conditions. The divergence among various researches might be mainly caused by different soil water flow conditions (Bristow et al., 2000; Cote et al., 2003; Gärdenäs et al., 2005). Superior to late-SPAM, RMAM obtained the highest coincidence degree between nutrients and roots (Figs. 1 and 5, Table 3), indicating the most favorable allocation of nutrients for root uptake. On 93 DAS in 2020, soil mineral N in the shallow, intermediate and deep layers of root zone accounted for 42%, 34% and 24% (Fig. 5A), respectively, which agreed well with root distribution (Fig. 1). Among the five schemes evaluated in the current study, the greatest nutrient uptake found under RMAM (Fig. 9) resulted in the most significant enhancement in cotton growth (Fig. 7), yield and fertilizer use efficiency (Fig. 8), and thus the least deep losses in leachate (Fig. 4B) and lowest soil residuals (Fig. 6). Compared to RMAM, although UMAM also applied fertilizer through three times, its worse performance might be resulted from insufficient nutrient supply to roots in the top zone, similar to that under early-SPAM.

Obviously, fertigation scheduling affects soil nutrient transport and distribution and further impacts nutrient uptake, as well as crop growth and yields (Haynes, 1985; Cote et al., 2003; Li et al., 2004; Hou et al., 2007). To enhance the coincidence degree between soil nutrients and roots, timing and rate were optimized for fertilizer injection based on root profile (RMAM). Compared to SPAM (T1-T3) or UMAM (T5), RMAM (T4) achieved the expected target to increase yield and fertilizer use efficiency by creating more advantageous soil nutrient conditions for root uptake, validating the feasibility for optimization. However, significant losses of mineral N and especially available K to deep soils with leachate still occurred. In addition, relative to soil mineral N and available K, available P still showed much lower coincidence degree with roots under RMAM (Table 3). Further improvement may be possible through:

1) Fully considering the effects of soil water and nutrient dynamics

Root-zone soil water and nutrient dynamics are purpose- and environment-dependent and change with crop growth, as well as increasing rooting depth. Thereupon, designed wetting depth and thus fertilizer application scheme should be correspondingly and timely adjusted. For example, following three designed soil wetting depths of 40 (for saving water), 60 and 80 cm (for leaching salt) combined with a definite rooting depth of 60 cm would require different fertigation schedules (e.g., application times, timing and rate). Unfortunately, the current RMAM has not yet considered the challenges posed by the dynamic relationship between rooting depth and designed soil wetting depth. Additionally, soil nutrient dynamics during fertigating process is affected inevitably by the factors impacting soil water flow (e.g., irrigation frequency, irrigation intensity, soil properties and initial soil water conditions), as well as nutrient types and initial soil nutrient conditions (Vanderborght and Vereecken, 2007; Sadeghi and Jones, 2012; Wang et al., 2017; Azad et al., 2020), which have also not been considered.

For example, frequency of irrigation events and rainfall are expected to influence not only water and nutrient profiles but also possibly soil oxygen and root distribution patterns (Wang et al., 2006; Rank and Vishnu, 2021). These could additionally explain discrepancies between results from various studies regarding effects of fertigation timing. In the present study, except the first event for germination, irrigation was applied about every 5–10 days at rates of 30–35 mm per event. Trends of increasing irrigation frequency with drip systems designed to increase both water uptake efficiency (Segal et al., 2006; Shao et al., 2009) and nutrient use efficiency (Ben-Gal and Dudley, 2003; Assouline et al., 2006), where theoretically the cotton in this study would receive about 10 mm of water every 2–3 days, would likely concentrate roots in shallow soil layers as well as lessen the horizontal transport of solutes. We suspect that the combined effects of increased irrigation frequency would not likely change the results or conclusions of this study, but it is a topic worthy of further research.

In order to deal with the mentioned challenges, it would be wise to numerically simulate soil water and nutrient dynamics under complicated conditions for screening and optimizing rational fertigation protocols (Hanson et al., 2006; Azad et al., 2018). Specific schemes are also obviously necessary for different nutrient types. For instance, for available P with poor mobility, a higher application percentage might be firstly adopted in the early stage of an irrigation event, in comparison to mobile nutrients such as mineral N and available K. Secondly, as shown in Fig. 5B and Table 3, increasing fertilizer application frequencies during a single irrigation event or implementing a continuous variable application method should be feasible to alleviate P accumulation in the upper soil layers (Clothier and Green, 1994; Ben-Gal and Dudley, 2003; Silber et al., 2003; Mohammad et al., 2004). Ben-Gal and Dudley (2003), in their study of P dynamics, found advantage of lower dripper flow rates and continuous fertilizer application throughout irrigation events in increasing P availability and use efficiency as sorption was minimized. Thirdly, other technical measures to enhance P mobility such as applying P activators (Lombi et al., 2005; Carter et al., 2009) can also be considered.

2) Exploring an effective index to accurately characterize root uptake activity

Essentially, RMAM intends to coordinate the distributions of soil nutrient supply and root uptake activity. In fact, it is very difficult to accurately characterize root uptake activity (Pierret et al., 2005; Shi and Zuo, 2009; Shi et al., 2013). Water uptake coefficient per unit root length is often assumed as a constant in the root zone, indicating a linearly proportional relationship between root water uptake rate and root length density under optimal water conditions (Feddes et al., 1978; Wu et al., 1999). Based on this hypothesis and a large number of available experimental data regarding root length density, the generalized quantitative description of NRLD as Eq. (1) (Zuo et al., 2013; Ning et al., 2015, 2019) was used to represent the distribution of root uptake activity in many previous studies (Shi et al., 2015, 2020, 2021), as well as in this study. However, research has shown that not all roots have uptake function, and the uptake activities of roots or various parts are different from each other. Relatively, younger roots are much more likely to actively absorb water than older roots (Slatyer, 1960; Gao et al., 1998; Pierret et al., 2005). In view of this, determining a fertilizer application scheme based on NRLD distribution might lead to a deviation between the profiles of soil nutrients and root uptake activity. Moreover, relative to root length, some recent studies have demonstrated more significant linearly proportional relationship between root uptake activity and root nitrogen mass (Shi and Zuo, 2009; Shi et al., 2013). Therefore, as an alternative of NRLD distribution, normalized root nitrogen mass density distribution might be more reasonably to characterize root nutrient uptake activity and to optimize fertilizer application scheme. However, corresponding experimental or statistical data are scarce, and further studies are needed.

5. Conclusions

Under the conditions developed in the current study, the fertilizer application schemes significantly influenced the transport of soil nutrients, deep leaching, residual contents, as well as the absorption of soil nutrients, crop growth and yield. Generally, SPAM caused significant nutrient accumulation in certain soil layers, depending on application timing and nutrient mobility, and UMAM produced a more uniform nutrient profile. Nevertheless, RMAM resulted in an optimal nutrient profile for root uptake, where more nutrients were in the upper soil layers with more roots. Therefore, RMAM significantly promoted crop nutrient uptake, growth and production, and reduced leachate loss and soil residue, beneficial for environmental protection and sustainable agricultural development. However, in addition to root length density, crop nutrient uptake is also affected by many other complicated purpose- and environment-dependent factors related with soil water/nutrient dynamics and root uptake activity. Further improvement is necessary for RMAM to take soil water/nutrient dynamics under various conditions into account and explore an effective index to accurately characterize root uptake activity.

Declaration of interest statement

The authors declare that we have no financial and personal relationships with other people or organizations that can inappropriately influence our work, there is no professional or other personal interest of any nature or kind in any product, service and/or company that could be construed as influencing the position presented in the manuscript entitled “Optimizing fertigation schemes based on root distribution”.

Data Availability

Data will be made available on request.

Acknowledgements

This work was financially supported by the National Natural Science Foundation of China (51790532); the Major Scientific and Technological Program of Xinjiang in China (2020A01002-3); the Natural Science Foundation of Xinjiang (2022D01D09); and the National Key Research and Development Program of China (2021YFD1900803).

References

Assouline, S., Möller, M., Cohen, S., Ben-Hur, M., Grava, A., Narkis, K., Silber, A., 2006. Soil-plant system response to pulsed drip irrigation and salinity: bell pepper case study. Soil Sci. Soc. Am. J. 70, 1556–1568. https://doi.org/10.2136/sssaj2005.0365.

Azad, N., Behmanesh, J., Rezaverdinejad, V., Abbasi, F., Navabian, M., 2018. Developing an optimization model in drip fertigation management to consider environmental issues and supply plant requirements. Agric. Water Manag. 208, 344–356. https://doi.org/10.1016/j.agwat.2018.06.030.

Azad, N., Behmanesh, J., Rezaverdinejad, V., Abbasi, F., Navabian, M., 2020. An analysis of optimal fertigation implications in different soils on reducing environmental impacts of agricultural nitrate leaching. Sci. Rep. 10, 1–15. https://doi.org/10.1038/s41598-020-64856-x.

Bar-Tal, A., Yermiyahu, U., Ben-Gal, A., 2020. Advances in fertigation techniques to optimize crop nutrition. In: Rengel, Z. (Ed.), Achieving Sustainable Crop Nutrition. Burleigh Dodds Science Publishing, Cambridge, UK, pp. 691–718. https://doi.org/10.19103/AS.2019.0062.28.

Ben-Gal, A., Dudley, L.M., 2003. Phosphorus availability under continuous point source irrigation. Soil Sci. Soc. Am. J. 67, 1449–1456. https://doi.org/10.2136/sssaj2003.1449.

Bristow, K.L., Cote, C.M., Thorburn, P.J., Cook, F.J., 2000. Soil wetting and solute transport in trickle irrigation systems. 6th Int. Micro Irrig. Congr. 1–9. Cape Town, South Africa, 22-27 October 2000.

Brown, R.L., Hangs, R., Schoenau, J., Bedard-Haughn, A., 2017. Soil nitrogen and phosphorus dynamics and uptake by wheat grown in drained prairie soils under three moisture scenarios. Soil Sci. Soc. Am. J. 81, 1496–1504. https://doi.org/10.2136/sssaj2017.01.0036.

Carter, C.M., van der Sloot, H.A., Cooling, D., 2009. pH-dependent extraction of soil and soil amendments to understand the factors controlling element mobility. Eur. J. Soil Sci. 60, 622–637. https://doi.org/10.1111/j.1365-2389.2009.01139.x.

Chen, S., Liu, C., 2002. Analysis of water movement in paddy rice fields (I) experimental studies. J. Hydrol. 260, 206–215. https://doi.org/10.1016/S0022-1694(01)00615-1.

Chen, S., Mao, X., Barry, D.A., Yang, J., 2019. Model of crop growth, water flow, and solute transport in layered soil. Agric. Water Manag. 221, 160–174. https://doi.org/10.1016/j.agwat.2019.04.031.

Chen, W., Hou, Z., Wu, L., Liang, Y., Wei, C., 2010. Effects of salinity and nitrogen on cotton growth in arid environment. Plant Soil 326, 61–73. https://doi.org/10.1007/s11104-008-9881-0.

Clothier, B.E., Green, S.R., 1994. Rootzone processes and the efficient use of irrigation water. Agric. Water Manag. 25, 1–12. https://doi.org/10.1016/0378-3774(94)90048-5.

Cote, C.M., Bristow, K.L., Charlesworth, P.B., Cook, F.J., Thorburn, P.J., 2003. Analysis of soil wetting and solute transport in subsurface trickle irrigation. Irrig. Sci. 22, 143–156. https://doi.org/10.1007/s00271-003-0080-8.

Donagemma, G.K., Ruiz, H.A., Alvarez V, V.H., Ferreira, P.A., Cantarutti, R.B., da Silva, A.T., Figueiredo, G.C., 2008. Distribution of ammonium, nitrate, potassium, and phosphorus in columns of fertigated latosols. Rev. Bras. Cienc. Solo 32, 2493–2504. https://doi.org/10.1590/S0100-06832008000600026.

Feddes, R.A., Kowalik, P.J., Zarandy, H., 1978. Simulation of Field Water Use and Crop Yeld. Simulation Monographs Pudoc., Wageningen, The Netherlands. https://doi.org/10.1097/00010694–198003000-00016.

Gao, S., Pan, W., Koenig, R.T., 1998. Integrated root system age in relation to plant nutrient uptake activity. Agron. J. 90, 505–510. https://doi.org/10.2134/agronj1998.00021962009000040011x.

Gärdenäs, A., Hopmans, J., Hanson, B.R., Simunek Jirka, J., 2005. Two-dimensional modeling of nitrate leaching for various fertigation scenarios under micro-irrigation. Agric. Water Manag. 74, 219–242. https://doi.org/10.1016/j.agwat.2004.11.011.

Goins, G.D., Russelle, M.P., 1996. Fine root demography in alfalfa (*Medicago sativa* L.). Plant Soil 185, 281–291. https://doi.org/10.1007/BF02257534.

Hanson, B.R., Šimůnek, J., Hopmans, J.W., 2006. Evaluation of urea–ammonium–nitrate fertigation with drip irrigation using numerical modeling. Agric. Water Manag. 86, 102–113. https://doi.org/10.1016/j.agwat.2006.06.013.

Haynes, R.J., 1985. Principles of fertilizer use for trickle irrigated crops. Fert. Res. 6, 235–255. https://doi.org/10.1007/BF01048798.

Hou, Z., Li, P., Li, B., Gong, J., Wang, Y., 2007. Effects of fertigation scheme on N uptake and N use efficiency in cotton. Plant Soil 290, 115–126. https://doi.org/10.1007/s11104-006-9140-1.

Hou, Z., Chen, W., Li, X., Xiu, L., Wu, L., 2009. Effects of salinity and fertigation practice on cotton yield and N-15 recovery. Agric. Water Manag. 96, 1483–1489. https://doi.org/10.1016/j.agwat.2009.04.019.

Kim, Y.X., Ranathunge, K., Lee, S., Lee, Y., Lee, D., Sung, J., 2018. Composite transport model and water and solute transport across plant roots: an update. Front. Plant Sci. 9, 193. https://doi.org/10.3389/fpls.2018.00193.

Li, J., Zhang, J., Rao, M., 2004. Wetting patterns and nitrogen distributions as affected by fertigation strategies from a surface point source. Agric. Water Manag. 67, 89–104. https://doi.org/10.1016/j.agwat.2004.02.002.

Liang, J., Shi, W., 2021. Poly-gamma-glutamic acid improves water-stable aggregates, nitrogen and phosphorus uptake efficiency, water-fertilizer productivity, and economic benefit in barren desertified soils of Northwest China. Agric. Water Manag. 245, 106551 https://doi.org/10.1016/j.agwat.2020.106551.

Liu, L., Wang, T., Lichun, W., Wu, X., Zuo, Q., Shi, J., Sheng, J., Jiang, P., Chen, Q., Ben-Gal, A., 2022. Plant water deficit index-based irrigation under conditions of salinity. Agric. Water Manag. 269, 107669 https://doi.org/10.1016/j.agwat.2022.107669.

Lombi, E., McLaughlin, M.J., Johnston, C., Armstrong, R.D., Holloway, R.E., 2005. Mobility, solubility and lability of fluid and granular forms of P fertiliser in calcareous and non-calcareous soils under laboratory conditions. Plant Soil 269, 25–34. https://doi.org/10.1007/s11104-004-0558-z.

Ma, H., Pu, S., Li, P., Niu, X., Wu, X., Yang, Z., Zhu, J., Yang, T., Hou, Z., Ma, X., 2021. Towards to understanding the preliminary loss and absorption of nitrogen and phosphorus under different treatments in cotton drip-irrigation in northwest Xinjiang. PLoS One 16, 0249730. https://doi.org/10.1371/journal.pone.0249730.

Makhdum, M.I., Pervez, H., Ashraf, M., 2007. Dry matter accumulation and partitioning in cotton (*Gossypium hirsutum* L.) as influenced by potassium fertilization. Biol. Fertil. Soils 43, 295–301. https://doi.org/10.1007/s00374-006-0105-6.

Mohammad, M.J., Hammouri, A., Ferdows, A.E., 2004. Phosphorus fertigation and preplant conventional soil application of drip irrigated summer squash. J. Agron. 3, 162–169. https://doi.org/10.3923/ja.2004.162.169.

Ning, S., Shi, J., Zuo, Q., Wang, S., Ben-Gal, A., 2015. Generalization of the root length density distribution of cotton under film mulched drip irrigation. Field Crop. Res. 177, 125–136. https://doi.org/10.1016/j.fcr.2015.03.012.

Ning, S., Chen, C., Zhou, B., Wang, Q., 2019. Evaluation of normalized root length density distribution models. Field Crop. Res. 242, 107604 https://doi.org/10.1016/j.fcr.2019.107604.

Ning, S., Zhou, B., Shi, J., Wang, Q., 2021. Soil water/salt balance and water productivity of typical irrigation schedules for cotton under film mulched drip irrigation in northern Xinjiang. Agric. Water Manag. 245, 106651 https://doi.org/10.1016/j.agwat.2020.106651.

Pierret, A., Moran, C.J., Doussan, C., 2005. Conventional detection methodology is limiting our ability to understand the roles and functions of fine roots. N. Phytol. 166, 967–980. https://doi.org/10.1111/j.1469-8137.2005.01389.x.

Rank, P.H., Vishnu, B., 2021. Pulse drip irrigation: a review. J. Pharmacogn. Phytochem. 10, 125–130.

Romano, N., Santini, A., 2002. Water retention and storage: field–field water capacity. In: Dane, J.H., Topp, G.C. (Eds.), Methods of Soil Analysis, Part 4 Physical Methods, No.5. Soil Science Society of America, Madison,WI, pp. 723–729.

Russo, D., 2016. Alternating irrigation water quality as a method to control solute concentrations and mass fluxes below irrigated fields: A numerical study. Water Resour. Res. 52, 3440–3456. https://doi.org/10.1002/2015WR018287.

Sadeghi, M., Jones, S.B., 2012. Scaled solutions to coupled soil-water flow and solute transport during the redistribution process. Vadose Zone J. 11 (4), 236–245. https://doi.org/10.2136/vzj2012.0023.

Schwab, G.J., Mullins, G.L., Burmester, C.H., 2000. Growth and nutrient uptake by cotton roots under field conditions. Commun. Soil Sci. Plant Anal. 31, 149–164. https://doi.org/10.1080/00103620009370426.

Segal, E., Ben-Gal, A., Shani, U., 2006. Root water uptake efficiency under ultra-high irrigation frequency. Plant Soil 282, 333–341. https://doi.org/10.1007/s11104-006-0003-6.

Shao, L., Zhang, X., Chen, S., Sun, H., Wang, Z., 2009. Effects of irrigation frequency under limited irrigation on root water uptake, yield and water use efficiency of winter wheat. Irrig. Drain. 58, 393–405. https://doi.org/10.1002/ird.442.

Shi, J., Zuo, Q., 2009. Root water uptake and root nitrogen mass of winter wheat and their simulations. Soil Sci. Soc. Am. J. 73, 1764–1774. https://doi.org/10.2136/sssaj2009.0002.

Shi, J., Ben-Gal, A., Yermiyahu, U., Wang, L., Zuo, Q., 2013. Characterizing root nitrogen uptake of wheat to simulate soil nitrogen dynamics. Plant Soil 363, 139–155. https://doi.org/10.1007/s11104-012-1299-z.

Shi, J., Li, S., Zuo, Q., Ben-Gal, A., 2015. An index for plant water deficit based on root-weighted soil water content. J. Hydrol. 522, 285–294. https://doi.org/10.1016/j.jhydrol.2014.12.045.

Shi, J., Wu, X., Wang, X., Zhang, M., Ben-Gal, A., 2020. Determining threshold values for root-soil water weighted plant water deficit index based smart irrigation. Agric. Water Manag. 230, 105979 https://doi.org/10.1016/j.agwat.2019.105979.

Shi, J., Wu, X., Zhang, M., Wang, X., Ben-Gal, A., 2021. Numerically scheduling plant water deficit index-based smart irrigation to optimize crop yield and water use efficiency. Agric. Water Manag. 248, 106774 https://doi.org/10.1016/j.agwat.2021.106774.

Silber, A., Xu, G., Levkovitch, I., Soriano, S., Bilu, A., Wallach, R., 2003. High fertigation frequency: the effects on uptake of nutrients, water and plant growth. Plant Soil 253, 467–477. https://doi.org/10.1023/A:1024857814743.

Simunek, J., Sejna, M., van Genuchten, M.T., 1999. The Hydrus-2D software package for simulating water flow and soulte transport in two-dimensional variably saturated media Version 2.0. U. S. Salin. Lab., Riverside, Calif.

Slatyer, R.O., 1960. Absorption of water by plants. Bot. Rev. 26, 331–392. https://doi.org/10.1007/BF02860807.

Tao, R., Wakelin, S.A., Liang, Y., Chu, G.X., 2017. Organic fertilization enhances cotton productivity, nitrogen use efficiency, and soil nitrogen fertility under drip irrigated field. Agron. J. 109, 2889–2897. https://doi.org/10.2134/agronj2017.01.0054.

van Genuchten, M.T., 1980. A closed-form equation for predicting the hydraulic conductivity of unsaturated soils. Soil Sci. Soc. Am. J. 44, 892–898. https://doi.org/10.2136/sssaj1980.03615995004400050002x.

Vanderborght, J., Vereecken, H., 2007. Review of dispersivities for transport modeling in soils. Vadose Zone J. 6, 29–52. https://doi.org/10.2136/vzj2006.0096.

Wang, D., Mo, Y., Li, G., Wilkerson, C.J., Hoogenboom, G., 2021. Improving maize production and decreasing nitrogen residue in soil using mulched drip fertigation. Agric. Water Manag. 251, 106871 https://doi.org/10.1016/j.agwat.2021.106871.

Wang, F., Kang, Y., Liu, S., 2006. Effects of drip irrigation frequency on soil wetting pattern and potato growth in North China Plain. Agric. Water Manag. 79, 248–264. https://doi.org/10.1016/j.agwat.2005.02.016.

Wang, H., Wu, L., Cheng, M., Fan, J., Zhang, F., Zou, Y., Chau, H.W., Gao, Z., Wang, X., 2018. Coupling effects of water and fertilizer on yield, water and fertilizer use efficiency of drip-fertigated cotton in northern Xinjiang, China. Field Crop. Res. 219, 169–179. https://doi.org/10.1016/j.fcr.2018.02.002.

Wang, J., Huang, Y., Long, H., Hou, S., Xing, A., Sun, Z., 2017. Simulations of water movement and solute transport through different soil texture configurations under negative-pressure irrigation. Hydrol. Process. 31, 2599–2612. https://doi.org/10.1002/hyp.11209.

Wu, J., Zhang, R., Gui, S., 1999. Modeling soil water movement with water uptake by roots. Plant Soil 215, 7–17. https://doi.org/10.1023/A:1004702807951.

Yang, F., Du, M., Tian, X., Eneji, A.E., Duan, L., Li, Z., 2014. Plant growth regulation enhanced potassium uptake and use efficiency in cotton. Field Crop. Res. 163, 109–118. https://doi.org/10.1016/j.fcr.2014.03.016.

Zong, R., Wang, Z., Zhang, J., Li, W., 2021. The response of photosynthetic capacity and yield of cotton to various mulching practices under drip irrigation in Northwest China. Agric. Water Manag. 249, 106814 https://doi.org/10.1016/j.agwat.2021.106814.

Zuo, Q., Zhang, R., Shi, J., 2013. Characterization of the root length density distribution of wheat using a generalized function. In: Timlin, D., Ahuja, L.R. (Eds.), Enhancing Understanding and Quantification of Soil-Root Growth Interactions. Advances in Agricultural Systems Modeling, pp. 93–117. https://doi.org/10.2134/advagricsystmodel4.c5.